

Published in final edited form as:

Nat Immunol. 2016 November ; 17(11): 1273–1281. doi:10.1038/ni.3552.

MUC1 modulates the tumor immune microenvironment through the engagement of Siglec-9

Richard Beatson¹, Virginia Tajadura-Ortega¹, Daniela Achkova², Gianfranco Picco¹, Theodora-Dorita Tsourouktsoglou¹, Sandra Klausning³, Matthew Hillier¹, John Maher², Thomas Noll³, Paul R. Crocker⁴, Joyce Taylor-Papadimitriou¹, and Joy M. Burchell^{1,5}

Breast Cancer Biology Group, Division of Cancer Studies, King's College London, Guy's Hospital, London, UK

²CAR Mechanics Group, Division of Cancer Studies, King's College London, Guy's Hospital, London, UK

³Cell Culture Technology Group, University of Bielefeld, Bielefeld, Germany

⁴School of Life Sciences, University of Dundee, UK

Abstract

Siglec-9 is a sialic acid binding lectin predominantly expressed on myeloid cells. Aberrant glycosylation occurs in essentially all types of cancers resulting in increased sialylation. Thus when MUC1 is expressed on cancer cells it is decorated by multiple short, sialylated O-linked glycans (MUC1-ST). Here we show that this cancer-specific MUC1 glycoform could, through the engagement of Siglec-9, educate myeloid cells to release factors associated with tumor microenvironment determination and disease progression. Moreover MUC1-ST induced macrophages to display a TAM-like phenotype with increased expression of PD-L1. MUC1-ST binding to Siglec-9 did not activate SHP-1/2 but surprisingly induced calcium flux leading to MEK-ERK activation. This work defines a critical role for aberrantly glycosylated MUC1 and identifies an activating pathway following Siglec-9 engagement.

Cancers have developed a plethora of mechanisms to evade the immune response including initiating a permissive local environment. For cancer cells to remodel their microenvironment they need to acquire changes that include the recruitment and education of monocytes, and the repolarization of resident macrophages¹. Macrophages are phenotypically plastic and factors produced by cancer cells can polarize macrophages to

Users may view, print, copy, and download text and data-mine the content in such documents, for the purposes of academic research, subject always to the full Conditions of use:http://www.nature.com/authors/editorial_policies/license.html#terms

⁵Corresponding author. joy.burchell@kcl.ac.uk.

Authors Contributions

R.B. and J.M.B. designed the study; R.B. performed the experiments with the assistance of D.A., G.P., T.-D.T., M.H.; V.T.-O. performed the qRT-PCR; S.K. and T.N. bulk cultured the CHO cells; P.R.C. and JM supplied reagents. J.T.-P. contributed to scientific discussion and approach. R.B. and J.M.B. wrote the manuscript with comments from all authors.

Competing Financial Interests

J.M.B. is a consultant to the company Palleon Pharma and P.R.C. is a scientific co-founder of Palleon Pharma. All other authors declare no competing financial interests.

become tumor-promoting. These tumor-educated macrophages promote the growth and invasion of cancer cells by contributing to all the stages involved in cancer dissemination, cumulating in metastasis²

Changes in glycosylation occur in essentially all types of cancers and changes in mucin-type O-linked glycans are the most prevalent aberrant glyco-phenotype when increased sialylation often occurs^{3,4}. The transmembrane mucin MUC1 is upregulated in breast and the majority of adenocarcinomas and, due to the presence of a variable number of tandem repeats that contain the O-linked glycosylation sites, can carry from 100 to over 750 O-glycans⁵. The aberrant glycosylation seen in cancer results in the multiple O-linked glycans carried by MUC1 being mainly short and sialylated^{3,6}, in contrast to the long, branched chains seen on MUC1 expressed by normal epithelial cells⁷. In carcinomas the aberrant O-linked glycosylation of MUC1 can alter the interaction of MUC1 with lectins of the immune system⁸ and thereby influence tumor-immune interplay. While it is clear that expression of MUC1 carrying short, sialylated core 1 glycans (NeuAc α _{2,3}Gal β ₁₋₃GalNAc; MUC1-ST) enhances tumor growth^{9,10}, the mechanisms underlying this increased growth are ill-defined. However, the immune system appears to play a role as syngeneic mouse tumor cells expressing MUC1-ST grow significantly faster in MUC1-transgenic mice than the same cells expressing MUC1 carrying branched core 2 glycans associated with normal glycosylation, while this differential growth is not seen in immunosuppressed mice⁹.

Siglecs (sialic acid-binding immunoglobulin-like lectins) are a family of sialic acid binding lectins, which, with the exception of Siglec-4, are expressed on various cells of the immune system¹¹. The cytoplasmic domains of most Siglecs contain immunoreceptor tyrosine-based inhibitory motifs (ITIMs), which recruit the tyrosine phosphatases, SHP-1 and/or SHP-2 (ref. 12) and so regulate the cells of the innate and adaptive immune response¹³. It has recently become clear that Siglecs play a role in cancer immune suppression, the hypersialylation seen in cancers inducing binding to these lectins^{14–16}. MUC1 expressed by cancer cells has been shown to bind to Siglec-9 resulting in the recruitment of β -catenin to the cytoplasmic tail of MUC1 inducing its translocation to the nucleus and increased tumor cell growth¹⁷. This work focused on the effect of the interaction with Siglec-9 on the MUC1 expressing cancer cells. In contrast we have investigated the effect of the interaction on the Siglec-9 expressing immune cells using a defined glycoform of MUC1 (ref. 18). Siglec-9 is predominantly expressed on myeloid cells and has a preference for sialic acid α _{2,3} linked to galactose¹⁹. Here we show that MUC1 carrying the sialylated core 1 glycan (MUC1-ST) a glycan not found on this mucin expressed by normal epithelial cells, binds to Siglec-9 on primary human monocytes and macrophages, and induces a unique secretome signature from each cell type. Moreover, when MUC1-ST binds to Siglec-9 expressed by primary macrophages a tumor-associated macrophage (TAM) phenotype is actively induced shown by the inhibition of CD8⁺ T cell proliferation and the upregulation of IDO (indoleamine 2,3-dioxygenase), CD163, CD206 and of the checkpoint ligand PD-L1 (programmed death ligand 1).

Results

MUC1-ST binds to Siglec-9 expressed by myeloid cells

To investigate the interaction of MUC1-ST with cells of the immune system, immune cell subsets were isolated from donor blood and incubated with biotinylated purified recombinant tumor-associated MUC1 glycoforms¹⁸ (Fig. 1a and Supplementary Fig. 1a). MUC1 carrying sialylated core-1 glycans (NeuAc α 2,3Gal β 1-3GalNAc; MUC1-ST), bound to primary monocytes and macrophages and acute myeloid leukemia (AML) lines (Fig. 1a–e). This interaction was lost upon neuraminidase treatment of MUC1-ST to give MUC1-T, demonstrating that the binding was dependent upon sialic acid (Fig. 1b–d). The binding also increased with time, maximum binding occurring at 5 hours, and with increased the concentration of MUC1-ST (Supplementary Fig. 1b,c) but was calcium independent (Fig. 1f). Moreover, the binding was enhanced when cells were pre-treated with neuraminidase (Supplementary Fig. 1d), which removes competing cis-binding sialic acid sites from the surface of the cells. This pattern is characteristic of binding to Siglec molecules¹¹ and indeed MUC1-ST bound recombinant Siglecs-3, 7, 9 and 10; with the greatest binding seen for Siglec-9 (Fig. 1g). Although Siglecs-3, 7 and 9 are expressed by monocytes and macrophages (Supplementary Fig. 1e), a blocking antibody to Siglec-9 inhibited 80-95% of the MUC1-ST binding to these cells (Fig. 1h,i; Supplementary Fig. 1f, Supplementary Table 1) indicating this is the dominant binding Siglec. It should be noted that this anti-Siglec-9 antibody can also act as an activating antibody as it recognizes the sialic acid binding site on Siglec-921. Importantly, Siglec-9 bound to the breast cancer cell line T47D that expresses MUC1 carrying sialylated core-1 glycans (Fig. 1j)²⁰. However, a multivalent polymer of sialylated core 1 glycans bound only weakly to monocytes and this interaction could not be inhibited with anti-Siglec-9 (Supplementary Fig. 1g). This finding suggests a contribution of the protein backbone to the binding specificity of Siglec-9, possibly by defining a specific spacing of the sialic acids. Thus MUC1-ST specifically binds to Siglec-9 on primary monocytes and macrophages.

MUC1-ST binding induces the secretion of various factors

To determine whether MUC1-ST binding induced a cellular response, we assayed for soluble factors released from cultured primary monocytes upon binding recombinant MUC1-ST. MUC1-ST induced monocytes to secrete several factors associated with inflammation and tumor progression (Fig. 2a and Supplementary Fig. 2a). We validated the induced secretion of interleukin 6 (IL-6), macrophage colony-stimulating factor (M-CSF) and plasminogen activator inhibitor-1 (PAI-1) by ELISA. Their induction was dependent upon recognition of sialic acid, as MUC1 carrying non-sialylated core-1 (MUC1-T) failed to induce such secretion (Fig. 2b,c,d) in addition blocking MUC1-ST binding using Siglec-9-specific antibody significantly decreased the secretion of these three factors (Fig. 2e,f,g). Some of the factors that were secreted upon MUC1-ST engagement of Siglec-9 have the potential to remodel the microenvironment by recruiting monocytes and neutrophils (CXCL5, CCL2, CCL3, CXCL1, IL-8 and PAI-1)^{22,23}, to induce angiogenesis (PAI-1, IL-8)^{24,25} and to degrade the extracellular matrix (MMP9, PAI-1)²⁶. Monocytes incubated with the breast cancer cell line T47D, which expresses MUC1-ST, also induced the release of PAI-1 (Fig. 2h). As a control, we used T47D cells that had been transfected with the

glycosyltransferase C2GnT1 (ref 20). C2GnT1 competes with the sialyltransferase that forms the ST glycan, resulting in expression of MUC1 carrying branched core-2 glycans that are representative of the glycosylation of MUC1 by normal mammary epithelial cells²⁰. The secretion of PAI-1 was significantly reduced when these transfected control cells were incubated with monocytes (Fig. 2h). In response to MUC1-ST, monocytes also produced pro-inflammatory nitric oxide (NO) (Fig. 2i), a product of the arginine processing enzyme²⁷. This release was partially reduced, although not significantly because of donor variation, with the Siglec-9 antibody (Fig. 2i). Thus Siglec-9 engagement by MUC1-ST induced the release of factors that can promote tumor growth and modulate the microenvironment.

MUC1-ST binding influences myeloid differentiation

As IL-6 and NO are known modulators of cellular differentiation^{28,29}, we assessed the effects of MUC1-ST on the differentiation of monocytes into macrophages or dendritic cells. Monocytes were differentiated into macrophages with M-CSF for seven days followed by lipopolysaccharide (LPS) and IFN- γ to give M(LPS+IFN- γ)³⁰ (historically defined as M1-like macrophages). When MUC1-ST was added at day 0 of the culture, the differentiated macrophages showed reduced surface expression of the co-stimulatory molecule CD86 (Fig. 3a,b) and secreted IL-12 was significantly reduced by over 10 fold (Fig. 3c). These significant phenotypic changes could at least be partially rescued by blocking antibodies to Siglec-9 or the IL-6 receptor (Fig. 3a-c). We induced primary monocytes to differentiate to macrophages in the presence or absence of MUC1-ST and then cultured with autologous T cells, which had been stimulated with anti-CD3 and anti-CD28. Proliferation of the CD8⁺ T cells, as measured by the decrease in eFluor670 dye by flow cytometry, was significantly inhibited when co-cultured with the macrophages differentiated from monocytes in the presence of MUC1-ST compare to those culture with macrophages differentiated from monocytes in the absence of MUC1-ST (Fig.3d). Moreover, these CD8⁺ T cells showed a lower level of activation as demonstrated by reduced expression of CD25 and CD69 (Fig. 3e,f). This inhibition of activation could be reversed by the presence of antibodies against Siglec-9 or IL-6 receptor α (IL-6R α) (Fig. 3f). The effect of the anti-Siglec-9 might be explained by Siglec-9 being expressed on a subset of T cells¹⁹. However, when monocytes were differentiated into macrophages in the presence of MUC1-ST and anti-Siglec-9, and then cultured with autologous T cells stimulated with anti-CD3 and anti-CD28, activation of the T cells was brought back to the isotype control (Fig. 3f, middle).

Monocytes differentiated into immature dendritic cells (DCs) with IL-4 and granulocyte-macrophage colony-stimulating factor (GM-CSF) in the presence of MUC1-ST displayed less expression of CD86 as compared to those differentiated to DCs in the absence of MUC1-ST (Supplementary Fig. 2b) and, when matured with LPS expressed less CD86 and CD83 (Supplementary Fig. 2c), as observed previously³¹. Antibodies to Siglec-9 and IL-6 significantly reversed this down-regulation of CD86 by immature and mature DCs (Supplementary Fig. 2d-f) and partially reversed the down-regulation of CD83 by mature DCs (data not shown). Thus, MUC1-ST binding to monocytes induces a pro-inflammatory phenotype that can recruit immune cells into the tumor, induce the secretion of factors

associated with tumor progression and induce the differentiation of monocytes into macrophages and dendritic cells with reduced CD8 stimulatory capacity.

MUC1-ST binding to macrophages induces a TAM phenotype

We assayed monocyte-derived macrophage secretion of proteins when these macrophages were treated with MUC1-ST (Fig. 4a). Similar to monocytes, macrophages increased secretion of M-CSF (Fig. 4b), PAI-1 (Fig. 4c) as well as the protease chitinase 3-like-1 (CHI3L1) (Fig. 4a). In addition, secretion of epidermal growth factor (EGF) was increased as compared to treatment of the macrophages with MUC1-T or no MUC1 (Fig. 4d). Production of these factors associated with tumor progression²⁴ was dependent upon Siglec-9 (Fig. 4e,f,g), although changes in EGF secretion were not significant due to donor variation. Importantly, as with monocytes, we detected increased secretion of PAI-1 after co-culturing macrophages with MUC1-ST-positive T47D cells (Fig. 4h). Moreover, when macrophages were cultured with T47D cells expressing MUC1 carrying branched core 2 glycans²⁰ (T47D core 2), the secretion of PAI-1 was significantly reduced as compared to T47D-ST (Fig. 4h). However, unlike MUC1-ST-treated monocytes, expression of chemokines associated with immunomodulation and cytokines were decreased or did not change (Fig. 4a). Thus, MUC1-ST, Siglec-9 'educated' monocytes and macrophages display unique secretomes.

Compared to controls, MUC1-ST-treated macrophages showed increased expression of mannose receptor (CD206) and the scavenger receptor CD163 (Fig. 5a). The expression of these makers is associated with tumor-associated macrophages³². Moreover, increased expression of the immune checkpoint ligand PD-L1 was observed (Fig. 5a), although only a minimal increase in PD-L2 was observed (data not shown). These phenotypic changes could all be rescued by blocking binding of MUC1-ST to macrophages with anti-Siglec-9 (Fig. 5a). In addition, treatment of macrophages with MUC1-ST increased the expression of the mRNA encoding indoleamine 2,3-dioxygenase (IDO) by 10-25 fold as compared to no MUC1-ST (Fig. 5b,c), which also could be rescued using a Siglec-9 antibody. IDO catalyzes the rate-limiting step in the metabolism of tryptophan and an increase in the tryptophan metabolite kynurenine was seen when macrophages were treated with MUC1-ST (Fig. 5d). The activity of IDO inhibits proliferation and induces apoptosis of T cells³³. Moreover increased expression of PD-L1 can engage the PD-1 receptor on activated T cells inhibiting their function³⁴. Macrophages that had been educated with MUC1-ST exhibited decreased ability to stimulate the proliferation and IFN- γ secretion of allogeneic CD8⁺ T cells, with these effects being inhibited with the Siglec-9 blocking antibody (Fig. 5e,f). To investigate the role of PD-L1 in the inhibition of CD8⁺ T cell proliferation we used the PD-1 blocking antibody pembrolizumab to inhibit the binding of PD-L1 to PD-1 on the T cells. However, we could not inhibit the reduction of T cell proliferation induced by MUC1-ST educated macrophages (Fig. 5g), nor could we rescue the decrease in IFN- γ observed when the interaction of PD-L1 with PD-1 was inhibited with pembrolizumab (Fig. 5h). Thus, in this *in vitro* system where the T cells are not responding to a specific antigen, PD-L1 does not contribute to the decrease in T cell proliferation induced by MUC1-ST-educated macrophages. This MUC1-ST-induced profile of expression and functional activity is

indicative of tumor-associated macrophages (TAMs), which play a role in promoting tumor progression^{35,36}.

MUC1-ST binding to Siglec-9 induces MEK-ERK activation

To investigate the intracellular effects of MUC1-ST binding we first assessed whether MUC1-ST was able to induce the phosphorylation of the inhibitory ITIM motif of Siglec-9, thereby inducing intracellular inhibitory signals¹². We hypothesized that this possibility was likely as the repeated glycans found on MUC1 should be able to crosslink Siglec-9. Surprisingly, instead of promoting phosphorylation, we found MUC1-ST inhibited the resting phosphorylation of Siglec-9 ITIM in monocytes and macrophages (Fig. 6a,b). Importantly, antibody-induced crosslinking of Siglec-9 did induce phosphorylation (Fig. 6a). Furthermore, phosphorylation of SHP-1, which is recruited by phosphorylated Siglec-9 (ref. 12), was not observed after MUC1-ST binding to Siglec-9 on primary monocytes (Fig. 6c). However, phosphorylation of SHP-1 was observed when Siglec-9 was activated via antibody cross-linking. No activation of SHP-2 was observed (data not shown). This finding is in contrast to the engagement of Siglec-9 with other, yet unknown, ligands present on tumor cells, where recruitment of SHP-1 was observed¹⁵. Moreover, in a murine tumor model Siglec-E, the murine Siglec with the most similarity to human Siglec-9, was associated with a decrease in alternatively activated macrophages¹⁵. Engagement of Siglecs has also been shown to inhibit calcium flux^{37,38}. We therefore investigated the triggering of a calcium flux when MUC1-ST engaged Siglec-9. When monocytes or macrophages were treated with MUC1-ST a calcium flux was induced that peaked at 30 s (Fig. 6d). This calcium flux was completely dependent on the engagement of Siglec-9 by MUC1-ST (Fig. 6e). A calcium flux was also observed when monocytes and T47D cells came into contact (Fig. 6f). This response could be inhibited by the Siglec-9 antibody and was not seen when T47D cells expressed normal branched core-2 glycans (Fig. 6f).

As binding of MUC1-ST to Siglec-9 did not induce phosphorylation associated with inhibitory signaling but rather induced a calcium flux, which is associated with activating signals³⁸, we investigated the downstream signaling after MUC1-ST binding to Siglec-9. To explore this possibility, the production of PAI-1 and M-CSF from MUC1-ST-educated monocytes and macrophages was assayed. As expected, the secretion of PAI-1 and M-CSF could be significantly inhibited by calcium channel inhibitor verapamil (Fig. 6g-j). Intracellular calcium flux can lead to activation of the MEK-ERK pathway³⁸. When monocytes or macrophages were incubated with MUC1-ST in the presence of the highly selective MEK inhibitor PD98059 (ref. 39), secretion of PAI-1 and M-CSF was significantly inhibited as compared to monocytes and macrophages incubated with MUC1-ST without the inhibitor (Fig. 6g-j). Moreover, the repression of T cell proliferation by MUC1-ST-treated macrophages could be partially overcome when MEK signaling was inhibited in the macrophages (Fig. 6k). Thus we have identified an activating role for Siglec-9 upon MUC1-ST binding.

Discussion

The majority of solid tumors contain infiltrating immune cells that are unable to eliminate the tumor and, in many cases, promote tumor progression¹. Tumor-associated macrophages are some of the most abundant immune cells to be found in tumors, their presence correlating with metastasis and poor prognosis^{35,36,40,41}. It has been proposed that for tumors to thrive they need to produce factors that can recruit and educate monocytes and repolarize resident macrophages into TAMs⁴¹. Here we have identified MUC1-ST as a myeloid modulating factor and as a driver of TAM formation demonstrated by the increased expression of CD206, CD163, IDO and PD-L1. MUC1-ST binding to Siglec-9 can increase expression of PD-L1 by macrophages is an important observation, as immune checkpoint inhibitors are showing extremely promising results in the clinic⁴². The degree of increase in expression of PD-L1 does differ with the healthy donors and ranges from 1.5-fold to over 7-fold. Highly relevant to this observation is that even modest effects on the expression of PD-L1 can lead to tumor regression in murine models⁴³ so changes up to 7 fold have the potential to be highly relevant to tumor growth. Additionally, these macrophages with a TAM-like phenotype can inhibit the proliferation and activation of CD8⁺ T cells. However the reduction in the proliferation of the T cells seen in our system does not appear to be due to the upregulation of PD-L1 on MUC1-ST educated macrophages as this could not be inhibited by the PD-1 blocking antibody, pembrolizumab. The PD-1–PD-L1 checkpoint is not active in the initial T cell activation stage but rather acts on effector cells recognizing antigen⁴⁴. Although the PD-L1 expressed by MUC1-ST–educated macrophages does not play a role in our *in vitro* assays where the proliferation of T cells is not antigen-specific, this finding does not exclude a role in cancer when tumors can be infiltrated with antigen-specific CD8⁺ T cells. Moreover, engagement of Siglec-9 on monocytes and macrophages by MUC1-ST induces the increased secretion of proteins involved in disease progression. Thus, this MUC1-ST–Siglec-9 axis plays an important role in orchestrating a tumor-permissive environment.

Aberrant glycosylation is a hallmark of cancer often resulting in increased sialylation^{3,4,6}, which has been shown to result in engagement of Siglecs^{14–16}. Individual Siglecs (except for Siglec-4) are expressed by different subset of cells within the immune system leading to an overlapping and complex pattern of expression¹¹. Siglec-9 is expressed by macrophages and monocytes, as well as by neutrophils, some B cells, a subset of T cells and a subset of NK cells. Ligands for Siglec-7 and Siglec-9 have been demonstrated on tumor cells^{14,15} and their engagement shown to inhibit NK activity^{14,16}. When tumor cells were incubated with neutrophils, the activation of the neutrophils was inhibited in a Siglec-9 dependent manner with increased killing of tumor cells in the presence of a Siglec-9 blocking antibody¹⁵. Mucins carry a very large number of O-linked glycans, the composition of which changes with malignancy resulting in the expression of shorter sialylated glycans⁴ with the potential to engage Siglecs. MUC16 has been identified as a ligand for Siglec-9 (ref. 45), as have mucins isolated from a colon carcinoma cell line⁴⁶. MUC1 however is the most widely expressed mucin in cancers derived from epithelial cells (adenocarcinomas) and the MUC1-ST glycoform is a dominant surface feature. MUC1 carrying undefined glycans could bind to Siglec-9 resulting in increased MUC1 signaling and growth of the MUC1-

expressing tumor cells *in vitro*. Infiltration of Siglec-9–expressing cells into MUC1-expressing tumors was observed *in vivo*¹⁷. However, this study did not investigate the effect on the immune cells of Siglec-9 engagement by MUC1. The availability of purified recombinant MUC1 carrying defined glycans¹⁸ has here allowed its use as a ligand to study the effects on myeloid cells of MUC1-ST binding to Siglec-9. The effects observed with this soluble MUC1-ST have been validated using the breast cancer cell line, T47D which expresses endogenous MUC1 carrying the ST glycan²⁰.

MUC1 can also be expressed by activated, but not resting, T cells, although this level of expression is at least 50 times lower than that expressed by breast cancer cells⁴⁷. MUC1 has also been seen on macrophages and dendritic cells. However, the O-linked glycosylation pattern of these cells changes with the activation state^{48,49} with activated T cells carrying core 2 glycans rather than the sialylated core 1 glycans (ST) that we show here binds Siglec-9.

In contrast to classical Siglec engagement, which results in the recruitment and activation of the phosphatases SHP-1 or SHP-2 (ref. 12), Siglec-9 engagement by MUC1-ST does not induce phosphorylation of this Siglec or SHP-1, but induces the transmission of activating signals. MUC1-ST binding to Siglec-9 on monocytes and macrophages induced changes that would impact on the microenvironment to promote tumor growth thereby acting as an immuno-modulator. The mechanism involved was demonstrated to be via the induction of a calcium flux leading to activation of the MEK-ERK pathway. Understanding the mechanisms that contribute to immune suppression by myeloid cells may help to develop new myeloid checkpoint inhibitors, such as anti-Siglec-9 immunotherapy.

The expression of the sialyltransferase ST3Gal-I is responsible for the addition of the sialic acid to the core 1 glycan forming ST6. This enzyme is overexpressed in breast and other carcinomas catalyzing the formation of short sialylated side chains. We have shown that in breast cancers COX-2 can increase the expression of ST3Gal-I⁵⁰. The principal metabolite of COX-2 is PGE₂ and COX-2 is induced by inflammatory mediators (e.g. IL-6). Thus the chronic inflammation induced by MUC1-ST binding to Siglec-9-positive myeloid cells would maintain the continued expression of the MUC1-ST glycoform via induced expression of COX-2. This positive feedback loop would maintain the induction of TAMs and the continued modulation of the microenvironment (Supplementary Fig. 3). Thus we have determined a vital function for aberrant O-linked glycosylation in tumor growth and progression.

On-Line Methods

Isolation and differentiation of immune subsets

Leukocytes cones were purchased from the National Blood Transfusion Service (NBTS, Tooting, UK) and centrifuged on a Ficoll gradient (Ficoll-Paque PREMIUM, GE Healthcare) at 400g. CD14⁺, CD19⁺, CD8⁺, CD4⁺ cells were isolated from PBMCs using microbeads (MACS system; Miltenyi Biotech) according to the manufacturer's instructions. Purity was assessed at >95% by staining with relevant antibodies. For ethical reasons, no information was supplied with these leukocyte cones. For the PD-L1 inhibition experiments

blood was taken with informed consent from healthy volunteers under ethical approval obtained for the National Research Ethics Service, South East Research Ethics Committee 1, study number 09/H0804/92.

To differentiate monocytes into macrophages, CD14⁺ cells were plated at a concentration of 1×10^6 /ml in AIM V medium (Lonza) with either 50 ng/ml recombinant human M-CSF or 50 ng/ml recombinant human GM-CSF (Bio-Techne). The cytokines were added every 3 days. The cells were incubated at 37 °C, 5% CO₂ for 7 days to fully differentiate, before being characterized as macrophages via phenotypic flow cytometric analysis. To further differentiate the macrophages the cells were treated with LPS and IFN- γ for 48 h to give M(LPS+IFN- γ)³⁰.

To differentiate monocytes into dendritic cells (moDC), CD14⁺ cells were plated at a concentration of 1×10^6 /ml in AIM V medium with 1500 U/ml recombinant human IL-4 (Bio-Techne) and 400 U/ml human GM-CSF (Bio-Techne) for 6 days to fully differentiate, before being characterised as immature DCs via phenotypic flow cytometric analysis (Epics XL, Beckman Coulter or FACSCalibur, BD Biosciences plus WinMDI or Cellquest software). MoDCs were matured using 1 μ g/ml LPS for 24 h.

Production of recombinant human MUC1 glycoforms

Recombinant secreted MUC1 consisting of 16 tandem repeats carrying sialylated core 1 and fused to mouse Ig was produced in CHO cells as described¹⁸. Concentrated supernatant was treated with 10 mg trypsin per mg MUC1-ST-IgG for 2 h (MUC1 tandem repeats are not sensitive to trypsin digestion) to remove the Ig. The treated supernatant was applied to a HiPrep 16/10 Q FF anion exchange column, which was washed to remove the unbound material with 20 column volumes of 50 mM Tris-HCl pH 8.0. The MUC1-ST was eluted as described¹⁸. The purity of the product was determined by giving a negative result in a mouse IgG ELISA, silver staining of SDS PAGE and an amino acid composition which was comparable to that reported previously¹⁸. All batches of purified MUC1-ST were tested for lack of endotoxin using the LAL assay (Lonza) as per manufacturer's instructions; TGF- β using an ELISA (Bio-Techne) as per manufacturer's instructions; Protease activity using the casein cleavage assay (Pierce/ThermoFisher) as per manufacturer's instructions. The product was quantitated either by amino acid analysis (Alta Bioscience) or using an HMFG2:HMFG2 sandwich ELISA against a previously quantified batch. It is important to note that the endotoxin concentrations of MUC1-ST 0.004-0.002 EU/ μ g, was well below the limits required for immunological experiments.

MUC1 carried core 1 glycans without sialylation, MUC1-T, was produced by dialyzing purified MUC1-ST in 50 mM NaAc pH 6.0, 4 mM CaCl₂ O/N at 4 °C, and then treating with 0.1 5 U/mg neuraminidase (NA) on agarose beads (Sigma) O/N at 23 °C and then dialyzed against PBS O/N. Cleavage of sialic acids was measured by HMFG2:lectin ELISA. Briefly 1 μ g/ml HMFG2 in PBS was bound to plastic O/N, before being blocked (1% BSA in PBS) and the samples (pre and post NA treatment) were loaded and incubated at 23 °C for 2 h. Sugars were analyzed using 1 μ g/ml biotinylated PNA (binds exposed galactose residues; does not bind ST) and 5 μ g/ml biotinylated MAA (binds α -2,3 linked sialic acids; does not bind T). Unglycosylated MUC1 was produced in CHO Id1D cells as described

previously⁸ without the addition of 1 mM GalNAc to the growth medium. Biotinylation of these glycoforms was performed as described previously⁸.

Binding of MUC1 glycoforms to cells

1×10^5 isolated / differentiated cells at 5×10^5 cells per ml were incubated for 4 h on ice with 10 μg of the appropriate biotinylated recombinant MUC1 glycoform in 0.5% BSA in PBS. Cells were washed in 0.5% BSA in PBS before 1:200 SAPE (Life Technologies) was added for 30 min on ice. Cells were washed and analyzed by flow cytometry or fluorescent microscopy (after cytospin). Blocking antibodies were used at 10 $\mu\text{g}/\text{ml}$.

Functional experiments

For functional experiments, isolated monocytes or monocyte derived macrophages were treated with 100 $\mu\text{g}/10^6$ cells MUC1-ST or MUC1-T (MUC1-ST with the sialic acid removed) for 4 h at 4 °C, washed and incubated at 37 °C for 48 h in AIM-V serum-free media.

To investigate the role of MUC1-ST on the differentiation of monocytes to macrophages, monocytes were incubated with MUC1-ST for 4 h at 4 °C and then differentiated in the presence of M-CSF. For blocking binding with anti-Siglec-9 antibody, monocytes were treated with 10 $\mu\text{g}/10^6$ anti-Siglec-9 or isotype control before being incubated with MUC1-ST for 4 h at 4 °C and then differentiated in the presence of M-CSF. To inhibit the action of IL-6, IL-6R α antibody, 10 $\mu\text{g}/\text{ml}$ Tocilizumab, was added every two days.

Binding of MUC1 glycoforms to recombinant Siglecs

Mouse anti human IgG was bound to plastic O/N and the plate was blocked using 1% BSA in PBSa. Recombinant human Siglec (3, 5, 7, 8, 9 and 10) fusion proteins were added at 2 $\mu\text{g}/\text{ml}$ for 2 h. After incubation with 2 $\mu\text{g}/\text{ml}$ biotinylated MUC1 glycoforms for 4 h, O.D was measured after the addition of streptavidin-HRP and substrate.

MLR and stimulation with anti-CD3 and anti-CD28

MUC1-ST educated macrophages were co-cultured for 48 h with either autologous CD8⁺ T cells ('AMLR'), in the presence of anti-CD3/CD28 beads, or allogeneic CD8⁺ T cells (MLR) labeled with eFluor® 670 (eBioscience) at a 1:1 ratio. eFluor® 670 is a protein dye that binds to primary amines and was used to measure proliferation through loss of fluorescence intensity by 2 after one division. CD8⁺ T cell proliferation, CD69/CD25 cell surface expression and IFN- γ production were measured using flow cytometry and ELISA (eBioscience).

For blocking PD-1, 10 $\mu\text{g}/\text{ml}$ Pembroluzumab or human IgG4 isotype control was added to isolated CD8⁺ T for 10 min before co-culturing with MUC1-ST educated macrophages for 72 h. After this period supernatant was taken for IFN- γ measurements.

Calcium flux

Monocytes pre-labeled with a intracellular calcium reporter (Fluo-4; Life Technologies) were treated with MUC1-ST, MUC1-T (100 $\mu\text{g}/10^6$ cells) or T47D monolayer, for 4 h at

4 °C. The cells were brought up to 37 °C and calcium flux was measured at 530 nm using a plate reader at the indicated time points. Where not indicated, time point was 60 s.

Phospho-Siglec 9 ELISA

Anti-human Siglec 9 was plated O/N on plastic before being blocked with 1% BSA in PBS. Clarified supernatant was added and incubated for 2 h. After incubation with 1 µg/ml biotinylated anti phospho-tyrosine, O.D (450 nm) was measured after the addition of streptavidin-HRP and substrate.

Cell lines, antibodies and other reagents

T47D cells obtained from the originator were cultured in RPMI 1640 (Lonza) supplemented with 100 units/ml penicillin, 100 µg/ml streptomycin, 2 mM L-glutamine and 10% heat-inactivated FCS (all Life Technologies). To maintain the cells authenticity cells were frozen as soon as possible after arrival to create a master bank. Cells were kept in culture for no longer than 10 weeks and expression of MUC1 was regularly checked. T47D cells transfected with C2GNT1 as described previously²⁰ were additionally cultured with 500 µg/ml G418. All cell lines were kept in culture for no longer than 12 weeks at a time.

Cell phenotype staining and neutralization was performed using the antibodies described in Supplementary Table 2. Cells were suspended in PBS + 0.5% BSA (2×10^5 cells/100 µl/sample) and incubated with MoAbs according to the manufacturer's instructions. At least 1×10^4 events were evaluated using either Epics XL, (Beckman Coulter) or FACSCalibur (BD Biosciences) flow cytometers. Analysis was performed using either WinMDI or Cellquest software.

Biotinylated polyacrylamide-ST (PAA-ST) was obtained from Glycotech. This is a synthetic carbohydrate probe in which the carbohydrate is incorporated into a polyacrylamide matrix thereby creating a 30 kDa multivalent polymer. The saccharide content is 20% and there are a nominal 20 trisaccharides per PAA and 4 biotin molecules. 10 µg/ml biotinylated PAA-ST was bound to monocytes and the binding visualized by flow cytometry using streptavidin-PE.

Protein arrays

Isolated monocytes were treated with $100 \mu\text{g}/10^6$ cells MUC1-ST for 4 h at 4 °C, washed and incubated at 37 °C for 48 h in AIM-V serum-free media. Supernatant was taken and cytokine production was assessed using an antibody capture protein array (Bio-Techne). Differentiated M-CSF macrophages were treated with $100 \mu\text{g}/10^6$ cells MUC1-ST for 4 h at 4 °C, washed, before being rapidly brought up to 37 °C for 5 min in PBS. Cells were immediately lysed on ice and clarified supernatant was used on a 59-phospho immunoreceptor array (Bio-Techne) according to manufacturer's instructions.

Nitric oxide

Supernatant was assessed using the Griess method according to the manufacturer's instructions (Biotium).

Kynurenine

60 µl supernatant was mixed with 30 µl 30% trichloroacetic acid (TCA) and incubated for 30 min at 50 °C. The supernatant was spun at 3000g and 50 µl was taken and mixed with 50 µl freshly prepared Ehrlich Reagent (2% p-dimethylaminobenzaldehyde in glacial acetic acid). After 10mins optical density was measured at 492 nm. Concentrations were calculated against a kynurenine standard curve.

ELISAs

ELISAs for IL-6, IL-12p70, TGF-β1, PAI-1, M-CSF, EGF, SHP2, phospho-SHP2 (Biotechne) were all carried out as per manufacturers instructions.

Immunoblots

Lysates were run on SDS PAGE (10% gel) before being transferred, blocked and probed with anti-SHP1 (Santa Cruz) or anti phospho SHP1 (Abcam) and appropriate secondary.

RNA isolation and qPCR

RNA was isolated from cells using RNeasy Mini kits (Qiagen). Contaminating DNA was removed with a DNase-free kit (Ambion). cDNA was synthesized using a SuperScript VILO kit (Invitrogen). Quantitative real-time PCR (qPCR) was carried out with cDNA using SYBR green-containing mastermix (Primer Design) using *PUM1* as a reference gene. The following oligonucleotides were used to test the expression of *IDO1*: F: 5'-ACAGACCACAAGTCACAGCG-3' R: 5'-GGACATCTCCATGACCTTTG-3' and *PUM1*: F: 5'-GATTATTCAGGCACGCAGGT-3' R: 5'-AGCAGCGCTGATGATGTATG-3'.

Statistical Analyzes

Sample size choice: The majority of the assays performed used either 3 donors to overcome donor variability.

Randomization and blinding statement: The majority of assays performed used blood from healthy volunteers. For all assays, excluding the PD-1 inhibition assay, these volunteers were provided by the NHS, with no associated information and were therefore blinded. There was therefore no need for randomisation of these donors.

Exclusion criteria: No 'outlier' tests were performed on any of our datasets.

Supplementary Material

Refer to Web version on PubMed Central for supplementary material.

Acknowledgements

This work was supported by grants from Breast Cancer Now (2011NovPR-43) with additional funding from the Medical Research Council. The authors acknowledge financial support from the Department the Experimental Cancer Medicine Centre at King's College London and by the National Institute for Health Research (NIHR) Biomedical Research Centre based at Guy's and St Thomas' NHS Foundation Trust and King's College London. The views expressed are those of the authors and not necessarily those of the NHS, the NIHR or the Department of Health.

The authors are grateful to V. Corrigan, King's College London, for the generous gift of Tocilizumab and to N. O'Reilly, The Crick Research Institute, London, for the lyophilization of samples.

References

1. Quail DF, Joyce JA. Microenvironmental regulation of tumor progression and metastasis. *Nat Med*. 2013; 19:1423–1437. [PubMed: 24202395]
2. Kitamura T, et al. Immune cell promotion of metastasis. *Nat Rev Immunol*. 2015; 15:73–86. [PubMed: 25614318]
3. Pinho SS, Reis CA. Glycosylation in cancer: mechanisms and clinical implications. *Nat Rev Cancer*. 2015; 15:540–555. [PubMed: 26289314]
4. Burchell JM, Mungul A, Taylor-Papadimitriou J. O-linked glycosylation in the mammary gland: changes that occur during malignancy. *J Mammary Gland Biol Neoplasia*. 2001; 6:355–364. [PubMed: 11547903]
5. Gendler SJ, et al. Molecular cloning and expression of human tumor-associated polymorphic epithelial mucin. *J Biol Chem*. 1990; 265:15286–15293. [PubMed: 1697589]
6. Burchell J, et al. An alpha2,3 sialyltransferase (ST3Gal I) is elevated in primary breast carcinomas. *Glycobiology*. 1999; 9:1307–1311. [PubMed: 10561455]
7. Lloyd KO, et al. Comparison of O-linked carbohydrate chains in MUC-1 mucin from normal breast epithelial cell lines and breast carcinoma cell lines. Demonstration of simpler and fewer glycan chains in tumor cells. *J Biol Chem*. 1996; 271:33325–33334. [PubMed: 8969192]
8. Beatson R, et al. The breast cancer-associated glycoforms of MUC1, MUC1-Tn and sialyl-Tn, are expressed in COSMC wild-type cells and bind the C-type lectin MGL. *PLoS One*. 2015; 10:e0125994. [PubMed: 25951175]
9. Mungul A, et al. Sialylated core-1-based O-linked glycans enhance the growth rate of mammary carcinoma cells in MUC1 transgenic mice. *Int J Oncol*. 2004; 25:937–943. [PubMed: 15375543]
10. Picco G, et al. Over-expression of ST3Gal-I promotes mammary tumorigenesis. *Glycobiology*. 2010; 20:1241–1250. [PubMed: 20534593]
11. Macauley MS, Crocker PR, Paulson JC. Siglec-mediated regulation of immune cell function in disease. *Nat Rev Immunol*. 2014; 14:653–666. [PubMed: 25234143]
12. Avril T, Floyd H, Lopez F, Vivier E, Crocker PR. The membrane-proximal immunoreceptor tyrosine-based inhibitory motif is critical for the inhibitory signaling mediated by Siglecs-7 and -9, CD33-related Siglecs expressed on human monocytes and NK cells. *J Immunol*. 2004; 173:6841–6849. [PubMed: 15557178]
13. Crocker PR. Siglecs and their roles in the immune system. *Nat Rev Immunol*. 2007; 7:255–266. [PubMed: 17380156]
14. Jandus C, et al. Interactions between Siglec-7/9 receptors and ligands influence NK cell-dependent tumor immunosurveillance. *J Clin Invest*. 2014; 124:1810–1820. [PubMed: 24569453]
15. Läubli H, et al. Engagement of myelomonocytic Siglecs by tumor-associated ligands modulates the innate immune response to cancer. *Proc Natl Acad Sci USA*. 2014; 111:14211–14216. [PubMed: 25225409]
16. Hudak JE, et al. Glycocalyx engineering reveals a Siglec-based mechanism for NK cell immunoevasion. *Nat Chem Biol*. 2014; 10:69–75. [PubMed: 24292068]
17. Tanida S, et al. Binding of the sialic acid-binding lectin, Siglec-9, to the membrane mucin, MUC1, induces recruitment of β -catenin and subsequent cell growth. *J Biol Chem*. 2013; 288:31842–31852. [PubMed: 24045940]
18. Bäckström M, et al. Recombinant MUC1 mucin with a breast cancer-like O-glycosylation produced in large amounts in Chinese-hamster ovary cells. *Biochem J*. 2003; 376:677–686. [PubMed: 12950230]
19. Zhang JQ, et al. Siglec-9, a Novel Sialic Acid Binding Member of the Immunoglobulin Superfamily Expressed Broadly on Human Blood Leukocytes. *J Biol Chem*. 2000; 275:22121–22126. [PubMed: 10801862]

20. Dalziel M, et al. The relative activities of the C2GnT1 and ST3Gal-I glycosyltransferases determine O-glycan structure and expression of a tumor-associated epitope on MUC1. *J Biol Chem.* 2001; 276:11007–11015. [PubMed: 11118434]
21. Carlin AF, et al. Molecular mimicry of host sialylated glycans allows a bacterial pathogen to engage neutrophil Siglec-9 and dampen the innate immune response. *Blood.* 2009; 113:3333–3336. [PubMed: 19196661]
22. Qian BZ, et al. CCL2 recruits inflammatory monocytes to facilitate breast cancer metastasis. *Nature.* 2011; 475:222–225. [PubMed: 21654748]
23. Thapa B, et al. Plasminogen activator inhibitor-1 regulates infiltration of macrophages into melanoma via phosphorylation of FAK-Tyr⁹²⁵. *Biochem Biophys Res Commun.* 2014; 450:1696–1701. [PubMed: 25063025]
24. McMahon GA, et al. Plasminogen activator inhibitor-1 regulates tumor growth and angiogenesis. *J Biol Chem.* 2001; 276:33964–33968. [PubMed: 11441025]
25. Bauerle KT, et al. Nuclear factor κ B-dependent regulation of angiogenesis, and metastasis in an in vivo model of thyroid cancer is associated with secreted interleukin-8. *J Clin Endocrinol Metab.* 2014; 99:E1436–E1444. [PubMed: 24758177]
26. Chen H, et al. Silencing of plasminogen activator inhibitor-1 suppresses colorectal cancer progression and liver metastasis. *Surgery.* 2015; 158:1704–1713. [PubMed: 26275833]
27. Thompson PA, et al. Environmental immune disruptors, inflammation and cancer risk. *Carcinogenesis.* 2015; 36:S232–S253. [PubMed: 26106141]
28. Oosterhoff D, et al. Tumor-mediated inhibition of human dendritic cell differentiation and function is consistently counteracted by combined p38 MAPK and STAT3 inhibition. *Oncoimmunology.* 2012; 1:649–658. [PubMed: 22934257]
29. Bogdan C. Nitric oxide synthase in innate and adaptive immunity: an update. *Trends Immunol.* 2015; 36:161–178. [PubMed: 25687683]
30. Murray PJ, et al. Macrophage activation and polarization: nomenclature and experimental guidelines. *Immunity.* 2014; 41:14–20. [PubMed: 25035950]
31. Rughetti A, et al. Recombinant tumor-associated MUC1 glycoprotein impairs the differentiation and function of dendritic cells. *J Immunol.* 2005; 174:7764–7772. [PubMed: 15944279]
32. Allavena P, Mantovani A. Immunology in the clinic review series; focus on cancer: tumour-associated macrophages; undisputed stars of the inflammatory tumour microenvironment. *Clin and Exp Immunol.* 2012; 167:195–205.
33. Forouzandeh F, et al. Differential immunosuppressive effect of indoleamine 2,3-dioxygenase (IDO) on primary human CD4+ and CD8+ T cells. *Mol Cell Biochem.* 2008; 309:1–7. [PubMed: 18008147]
34. Giancchetti E. Recent insights into the role of the PD-1/PD-L1 pathway in immunological tolerance and autoimmunity. *Autoimmun Rev.* 2013; 12:1091–100. [PubMed: 23792703]
35. Sousa S, et al. Human breast cancer cells educate macrophages toward the M2 activation status. *Breast Cancer Res.* 2015; 17:101. [PubMed: 26243145]
36. Qian BZ, Pollard JW. Macrophage diversity enhances tumor progression and metastasis. *Cell.* 2010; 141:39–45. [PubMed: 20371344]
37. Paul SP, Taylor LS, Stansbury EK, McVicar DW. Myeloid specific human CD33 is an inhibitory receptor with differential ITIM function in recruiting the phosphatases SHP-1 and SHP-2. *Blood.* 2000; 96:483–90. [PubMed: 10887109]
38. Christo SN, Diener KR, Hayball JD. The functional contribution of calcium ion flux heterogeneity in T cells. *Immunol and Cell Biology.* 2015; 93:694–704.
39. Dudley DT, et al. A synthetic inhibitor of the mitogen-activated protein kinase cascade. *Proc Natl Acad Sci USA.* 1995; 92:7686–7689. [PubMed: 7644477]
40. Xuan QJ, et al. Tumor-associated macrophages are correlated with tamoxifen resistance in the postmenopausal breast cancer patients. *Pathol Oncol Res.* 2014; 20:619–624. [PubMed: 24414992]
41. Noy R, Pollard JW. Tumor-associated macrophages: from mechanisms to therapy. *Immunity.* 2014; 41:49–61. [PubMed: 25035953]

42. Garon EB, et al. Pembrolizumab for the treatment of non-small cell lung cancer. *N Engl J Med*. 2015; 372:2018–2028. [PubMed: 25891174]
43. Casey SC, et al. MYC regulates the antitumour immune response through CD47 and PD-L1. *Science*. 2016; 352:227–231. [PubMed: 26966191]
44. Pardoll DM. The blockade of immune checkpoints in cancer immunotherapy. *Nature Rev Cancer*. 2012; 12:252–264. [PubMed: 22437870]
45. Belisle JA, et al. Identification of Siglec-9 as the receptor for MUC16 on human NK cells, B cells, and monocytes. *Mol Cancer*. 2010; 9:118. [PubMed: 20497550]
46. Ohta M, et al. Immunomodulation of monocyte-derived dendritic cells through ligation of tumor-produced mucins to Siglec-9. *Biochem Biophys Res Commun*. 2010; 402:663–669. [PubMed: 20971061]
47. Correa I, et al. Responses of human T cells to peptides flanking the tandem repeat and overlapping the signal sequence of MUC1. *Int J Cancer*. 2005; 115:760–768. [PubMed: 15729696]
48. Priatel JJ, et al. The ST3Gal-I sialyltransferase controls CD8+ T lymphocyte homeostasis by modulating O-glycan biosynthesis. *Immunity*. 2000; 12:273–283. [PubMed: 10755614]
49. Julien S, et al. Sialyl-Lewis(x) on P-selectin glycoprotein ligand-1 is regulated during differentiation and maturation of dendritic cells: a mechanism involving the glycosyltransferases C2GnT1 and ST3Gal I. *J Immunol*. 2007; 179:5701–5710. [PubMed: 17947642]
50. Sproviero D, Julien S, Burford B, Taylor-Papadimitriou J, Burchell JM. Cyclooxygenase-2 enzyme induces the expression of the α -2,3-sialyltransferase-3 (ST3Gal-I) in breast cancer. *J Biol Chem*. 2012; 287:44490–44497. [PubMed: 23275522]
51. Hartnell A, et al. Characterization of human sialoadhesin, a sialic acid binding receptor expressed by resident and inflammatory macrophage populations. *Blood*. 2001; 97:288–96. [PubMed: 11133773]
52. Ishida A, et al. Negative regulation of Toll-like receptor-4 signaling through the binding of glycosylphosphatidylinositol-anchored glycoprotein, CD14, with the sialic acid-binding lectin, CD33. *J Biol Chem*. 2014; 289:25341–50. [PubMed: 25059667]
53. Varchetta S, et al. Engagement of Siglec-7 receptor induces a pro-inflammatory response selectively in monocytes. *PLoS One*. 2012; 7:e45821. [PubMed: 23029261]
54. Carlin AF, et al. Molecular mimicry of host sialylated glycans allows a bacterial pathogen to engage neutrophil Siglec-9 and dampen the innate immune response. *Blood*. 2009; 113:3333–6. [PubMed: 19196661]
55. Tran TT, et al. Luminal lipid regulates CD36 levels and downstream signaling to stimulate chylomicron synthesis. *J Biol Chem*. 2011; 286:25201–10. [PubMed: 21610069]
56. Allen MD, et al. Altered microenvironment promotes progression of preinvasive breast cancer: myoepithelial expression of α v β 6 integrin in DCIS identifies high-risk patients and predicts recurrence. *Clin Cancer Res*. 2014; 20:344–57. [PubMed: 24150233]
57. Kishihara K, et al. Normal B lymphocyte development but impaired T cell maturation in CD45-exon6 protein tyrosine phosphatase-deficient mice. *Cell*. 1993; 74:143–56. [PubMed: 8334701]
58. Mihara M, et al. Tocilizumab inhibits signal transduction mediated by both mL-6R and sIL-6R, but not by the receptors of other members of IL-6 cytokine family. *Int Immunopharmacol*. 2005; 5(12):1731–40. [PubMed: 16102523]
59. Hamid O, et al. Safety and tumor responses with lambrolizumab (anti-PD-1) in melanoma. *N Engl J Med*. 2013; 369(2):134–44. [PubMed: 23724846]
60. Angelucci C, et al. Stearoyl-CoA desaturase 1 and paracrine diffusible signals have a major role in the promotion of breast cancer cell migration induced by cancer-associated fibroblasts. *Br J Cancer*. 2015; 112(10):1675–86. [PubMed: 25880005]
61. Hengartner NE, et al. Crucial role of IL1beta and C3a in the in vitro-response of multipotent mesenchymal stromal cells to inflammatory mediators of polytrauma. *PLoS One*. 2015; 10(1):e0116772. [PubMed: 25562599]
62. Chang TP, et al. Bortezomib inhibits expression of TGF- β 1, IL-10, and CXCR4, resulting in decreased survival and migration of cutaneous T cell lymphoma cells. *J Immunol*. 2015; 194(6): 2942–53. [PubMed: 25681335]

63. Zou Y, et al. NKP30-B7-H6 Interaction Aggravates Hepatocyte Damage through Up-Regulation of Interleukin-32 Expression in Hepatitis B Virus-Related Acute-On-Chronic Liver Failure. *PLoS One*. 2015; 10(8):e0134568. [PubMed: 26241657]
64. Hoyer JD, et al. CD33 detection by immunohistochemistry in paraffin-embedded tissues: a new antibody shows excellent specificity and sensitivity for cells of myelomonocytic lineage. *Am J Clin Pathol*. 2008; 129(2):316–23. [PubMed: 18208813]
65. Avril T, et al. The membrane-proximal immunoreceptor tyrosine-based inhibitory motif is critical for the inhibitory signaling mediated by Siglecs-7 and -9, CD33-related Siglecs expressed on human monocytes and NK cells. *J Immunol*. 2004; 173(11):6841–9. [PubMed: 15557178]
66. Llinàs L, et al. Expression profiles of novel cell surface molecules on B-cell subsets and plasma cells as analyzed by flow cytometry. *Immunol Lett*. 2011; 134(2):113–21. [PubMed: 20951740]
67. Kivi E, et al. Human Siglec-10 can bind to vascular adhesion protein-1 and serves as its substrate. *Blood*. 2009; 114(26):5385–92. [PubMed: 19861682]
68. Liu J, et al. CD14+HLA-DRlow/- expression: A novel prognostic factor in chronic lymphocytic leukemia. *Oncol Lett*. 2015; 9(3):1167–1172. [PubMed: 25663875]
69. Perussia B, et al. A human NK and K cell subset shares with cytotoxic T cells expression of the antigen recognized by antibody OKT8. *J Immunol*. 1983; 131(1):223–31. [PubMed: 6408172]
70. Kornum BR, et al. Common variants in P2RY11 are associated with narcolepsy. *Nat Genet*. 2011; 43(1):66–71. [PubMed: 21170044]
71. Spaan M, et al. Frequencies of Circulating MAIT Cells Are Diminished in Chronic HCV, HIV and HCV/HIV Co-Infection and Do Not Recover during Therapy. *PLoS One*. 2016; 11(7):e0159243. [PubMed: 27416100]
72. Van Rhijn I, et al. Human autoreactive T cells recognize CD1b and phospholipids. *Proc Natl Acad Sci U S A*. 2016; 113(2):380–5. [PubMed: 26621732]
73. Sarrabayrouse G, et al. CD4CD8 $\alpha\alpha$ lymphocytes, a novel human regulatory T cell subset induced by colonic bacteria and deficient in patients with inflammatory bowel disease. *PLoS Biol*. 2014; 12(4):e1001833. [PubMed: 24714093]
74. den Hartog G, et al. Modulation of human immune responses by bovine interleukin-10. *PLoS One*. 2011; 6(3):e18188. [PubMed: 21464967]
75. Weaver EA, et al. T-cell-biased immune responses generated by a mucosally targeted adenovirus- σ 1 vaccine. *Mucosal Immunol*. 2012; 5(3):311–9. [PubMed: 22377931]
76. Ball MS, et al. CDDO-Me Redirects Activation of Breast Tumor Associated Macrophages. *PLoS One*. 2016; 11(2):e0149600. [PubMed: 26918785]
77. Kostic I, et al. Lysophosphatidic acid enhances survival of human CD34(+) cells in ischemic conditions. *Sci Rep*. 2015; 5:16406. [PubMed: 26553339]
78. Lolmede K, et al. Inflammatory and alternatively activated human macrophages attract vessel-associated stem cells, relying on separate HMGB1- and MMP-9-dependent pathways. *J Leukoc Biol*. 2009; 85(5):779–87. [PubMed: 19197071]
79. Jutz S, et al. Assessment of costimulation and coinhibition in a triple parameter T cell reporter line: Simultaneous measurement of NF- κ B, NFAT and AP-1. *J Immunol Methods*. 2016; 430:10–20. [PubMed: 26780292]
80. Berry N, et al. The prognostic value of the monoclonal antibodies HMFG1 and HMFG2 in breast cancer. *Br J Cancer*. 1985; 51(2):179–86. [PubMed: 2578285]
81. Strauss G, et al. CD95 c-stimulation blocks activation of naïve T cells by inhibiting T cell receptor signaling. *J Exp Med*. 2009; 206:1379–1393. [PubMed: 19487421]
82. Abbonante V, et al. Discoidin domain receptor 1 protein is a novel modulator of megakaryocyte-collagen interactions. *J Biol Chem*. 2013; 288:16738–46. [PubMed: 23530036]
83. As assayed by manufacturer https://www.rndsystems.com/products/phospho-tyrosine-biotinylated-antibody-179003_bam1676

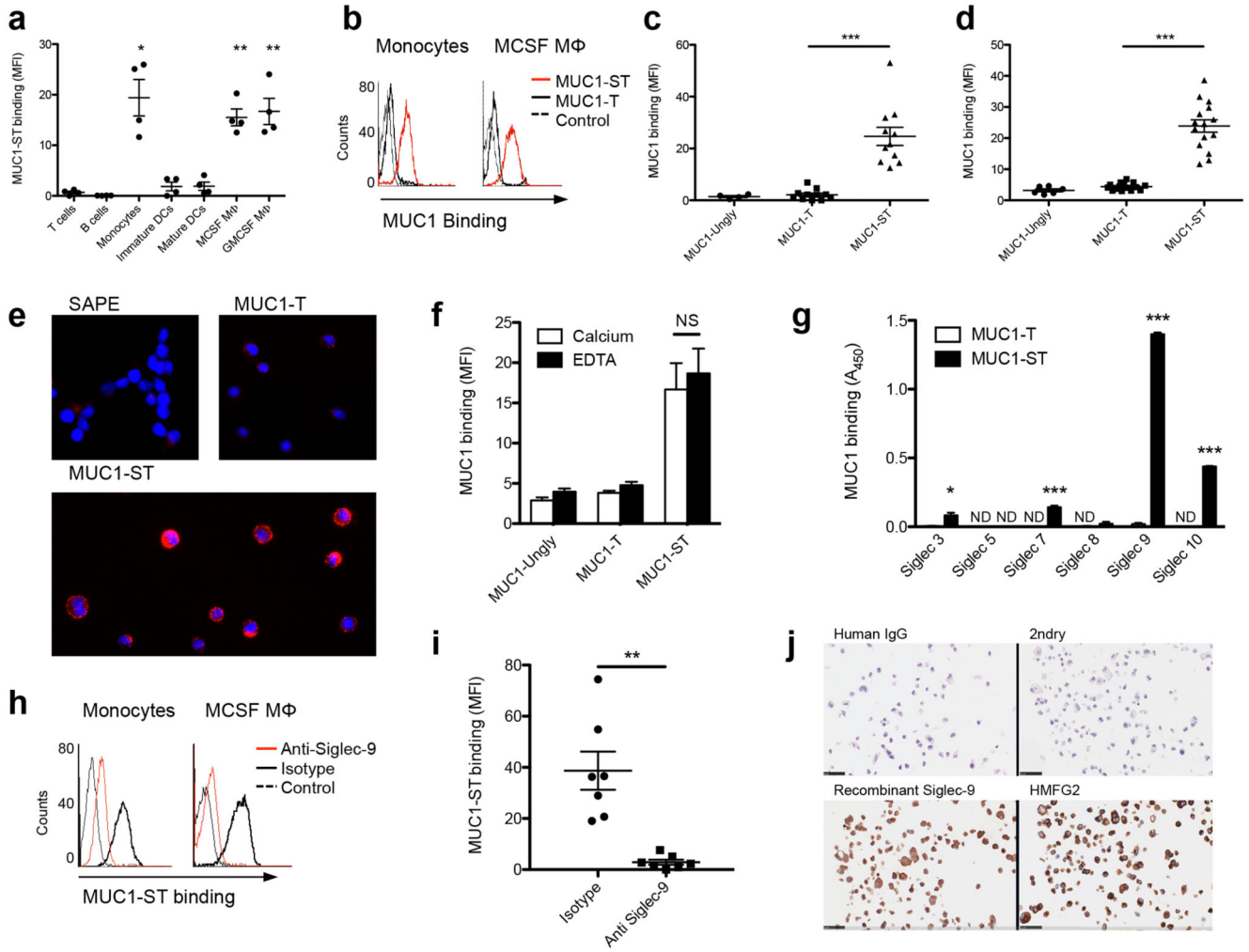


Figure 1. MUC1 carrying sialylated core-1 glycans (MUC1-ST) binds to primary monocytes and macrophages through Siglec-9. (a) Pooled flow cytometric analysis (MFI, mean fluorescence intensity) of isolated or differentiated immune subsets from healthy donors incubated with 10 μ g/ml biotinylated MUC1-ST. (b) Flow cytometry histograms of MUC1-ST and non-sialylated MUC1-T binding to primary monocytes and monocyte-derived macrophages and (c,d) bar graphs summarizing the data from multiple independent donors (MUC1-Ungly, unglycosylated MUC1). (e) U937 cells incubated with MUC1-ST or MUC1-T and visualized using fluorescent microscopy. (f) Pooled flow cytometric analysis (MFI) of monocytes binding to MUC1 glycoforms in the presence of Ca^{2+} or EDTA. (g) Binding of MUC1 glycoforms to Siglec fusion proteins. (h) Flow cytometry histograms of MUC1-ST binding to monocytes or macrophages after pre-incubation with anti-Siglec-9 or isotype control and (i) dot plots summarizing the data with monocytes from multiple independent donors. (j) Fixed T47D cells stained with human Siglec-9-IgG fusion or an anti-MUC1 (HMFG2). Scale bars represent 25 μ m. Data are from 4 independent donors (a); $N=11$ independent donors for MUC1-ST and MUC1-T, $N=4$ for MUC1-Ungly (c,d); Representative of 6 experiments showing the same results (e); $N=3$ independent donors (f);

Representative of 2 experiments, each done in triplicate, statistics refer to the technical triplicates (**g**); Representative of 7 independent donors; $N=7$ independent donors (**i**); Representative of 2 experiments showing similar results (**j**). Data shown are the mean and s.e.m. $P = * < 0.05$, $** < 0.01$, $*** < 0.001$, as determined by Student's paired t -test (**a,c,d,f,i**), or unpaired t -test (**g**).

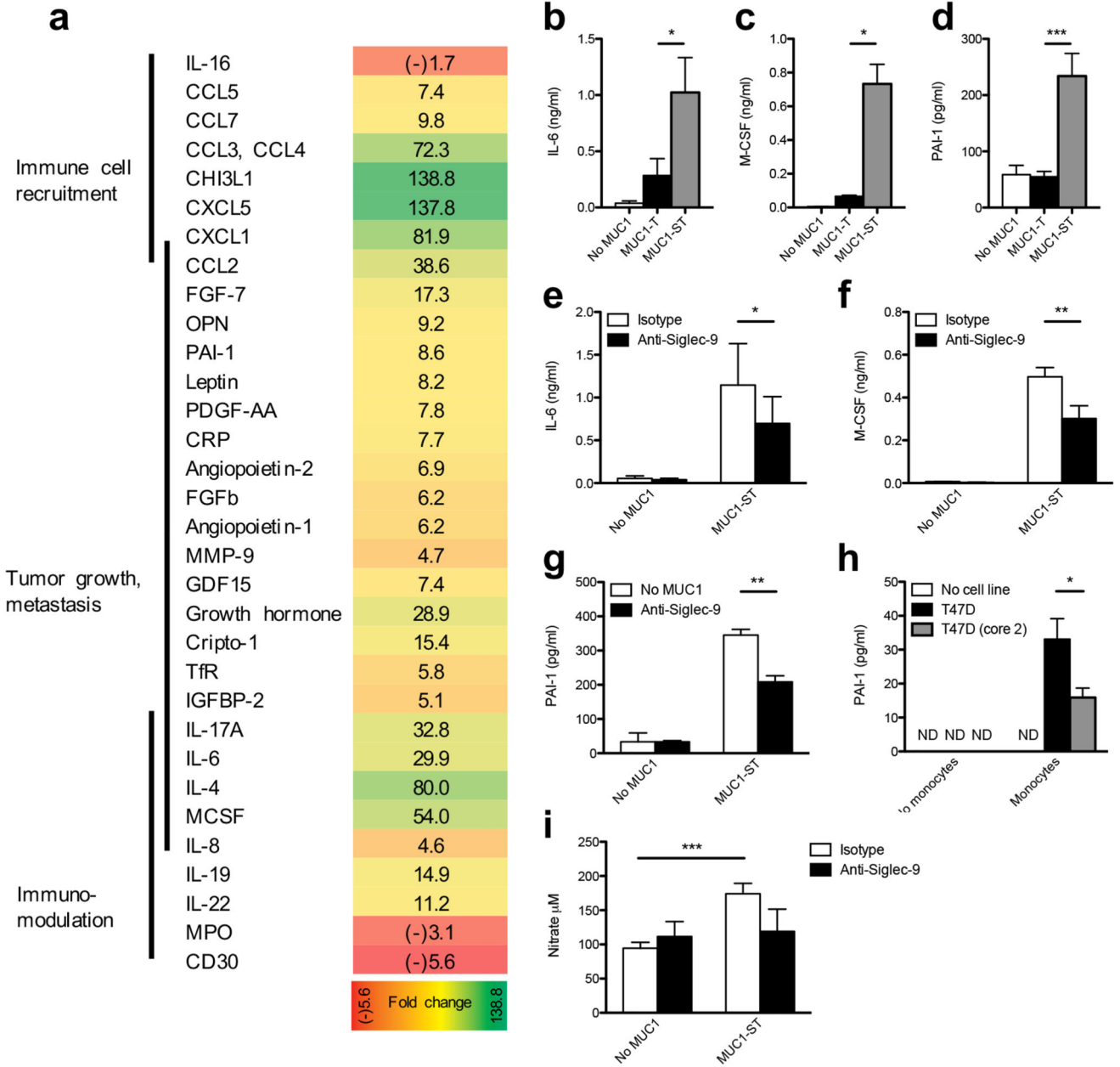


Figure 2. MUC1-ST induces monocytes to secrete factors associated with tumor progression in a Siglec-9-dependent manner. **(a)** The secretome from isolated primary monocytes treated with MUC1-ST clustered into functional groups. Figures represent fold change from untreated cells. Validation by ELISA of IL-6, M-CSF and PAI-1 released by primary monocytes in response to MUC1-ST, in a sialic acid **(b,c,d)** and Siglec-9 **(e,f,g)** dependent manner. **(h)** PAI-1 secreted by primary monocytes incubated with T47D cells and as a control T47D cells engineered to carry normal extended core 2 O-linked glycans (T47D (core 2)). **(i)** Nitric oxide release by monocytes after incubation with MUC1-ST in the presence or absence of anti-Siglec-9. Data is from 1 donor **(a)**; *N*=19 independent donors for

MUC1-ST and No MUC1, N=6 for MUC1-T (**b**); N=7 independent donors for MUC1-ST and No MUC1, N=3 for MUC1-T (**c**); N=8 independent donors for MUC1-ST and No MUC1, N=6 for MUC1-T (**d**); N=12 independent donors (**e**); N=4 independent donors (**f**); N=3 independent donors (**g**); N=2 independent experiments with technical triplicates, statistics refer to technical triplicates (**h**). N=13 (no MUC1/MUC1-ST), N=4 (isotype/anti-Siglec-9) (**i**).

Data shown are the mean and s.e.m. $P = * < 0.05$, $** < 0.01$, $*** < 0.001$, as determined by Student's paired *t*-test (b,c,d,e,f,g,i), or unpaired *t*-test (h).

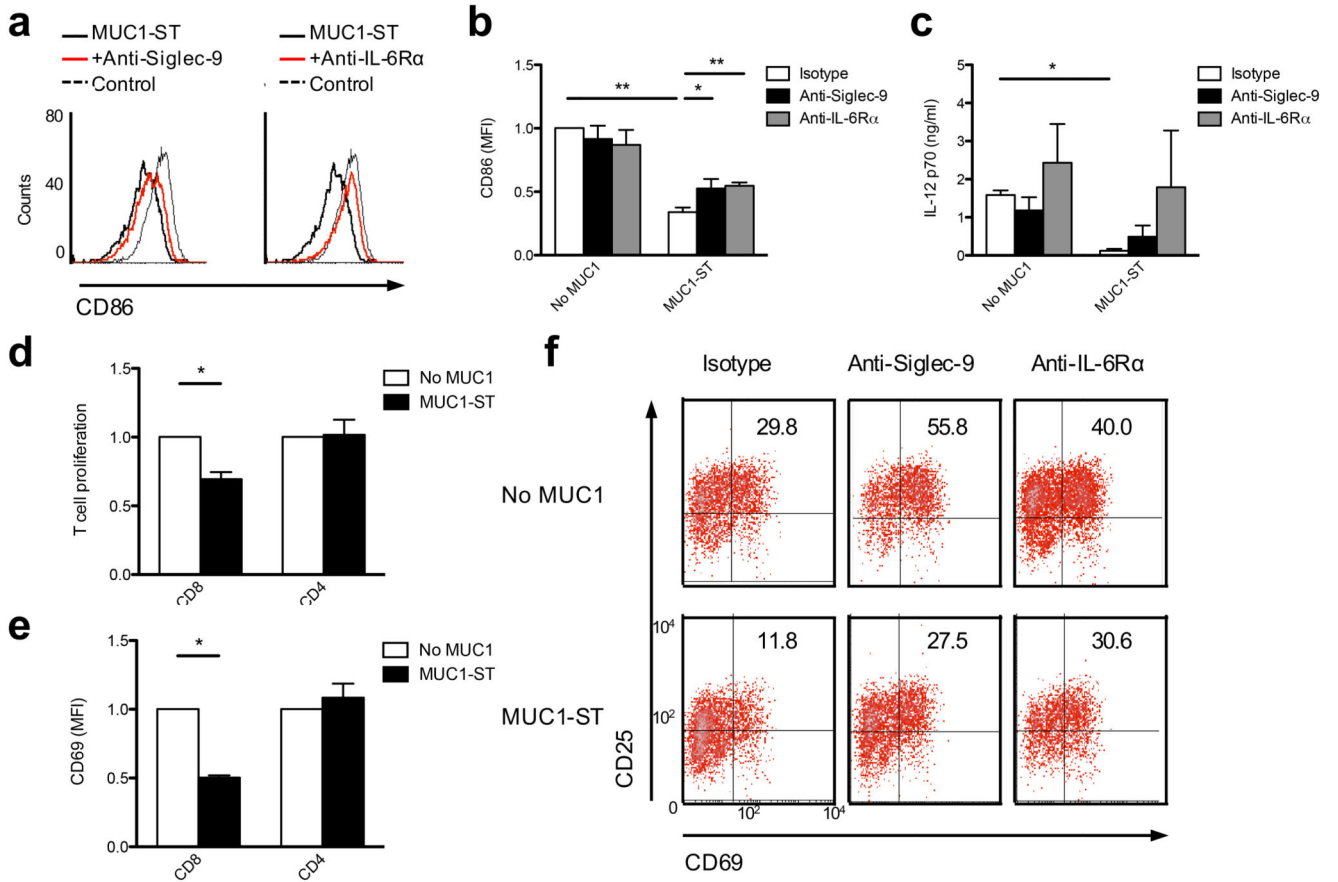


Figure 3.

MUC1-ST engagement of Siglec-9 during the differentiation of monocytes into inflammatory macrophages results in the generation of dysfunctional cells. **(a)** Flow cytometry histograms showing CD86 expression by LPS & IFN γ differentiated M-CSF macrophages after treatment with MUC1-ST on day 0 in the presence of isotype control or anti-Siglec-9 or anti-IL-6R α and **(b)** bar graphs summarizing the data from multiple independent donors. **(c)** IL-12 p70 release from macrophages treated as in (a,b). **(d,e,f)** Day 0 MUC1-ST treated M-CSF macrophages were co-cultured with autologous CD8 $^+$ or CD4 $^+$ T cells in the presence of anti-CD3 and anti-CD28 beads and proliferation **(d)** or expression of CD69 **(e)** were measured by flow cytometric analysis. **(f)** Density plots showing % of CD69 $^+$ CD25 $^+$ CD8 $^+$ T cells co-cultured with autologous M-CSF macrophages treated with MUC1-ST and antibody (isotype, anti-Siglec-9 or anti -L-6R α). $N=3$ independent donors **(b,c,d,e)**; Representative data from 3 independent donors showing similar results **(f)**. Data shown are the mean and s.e.m. $P = * < 0.05$, $** < 0.01$, as determined by Student's paired t -test **(b,c,d,e)**.

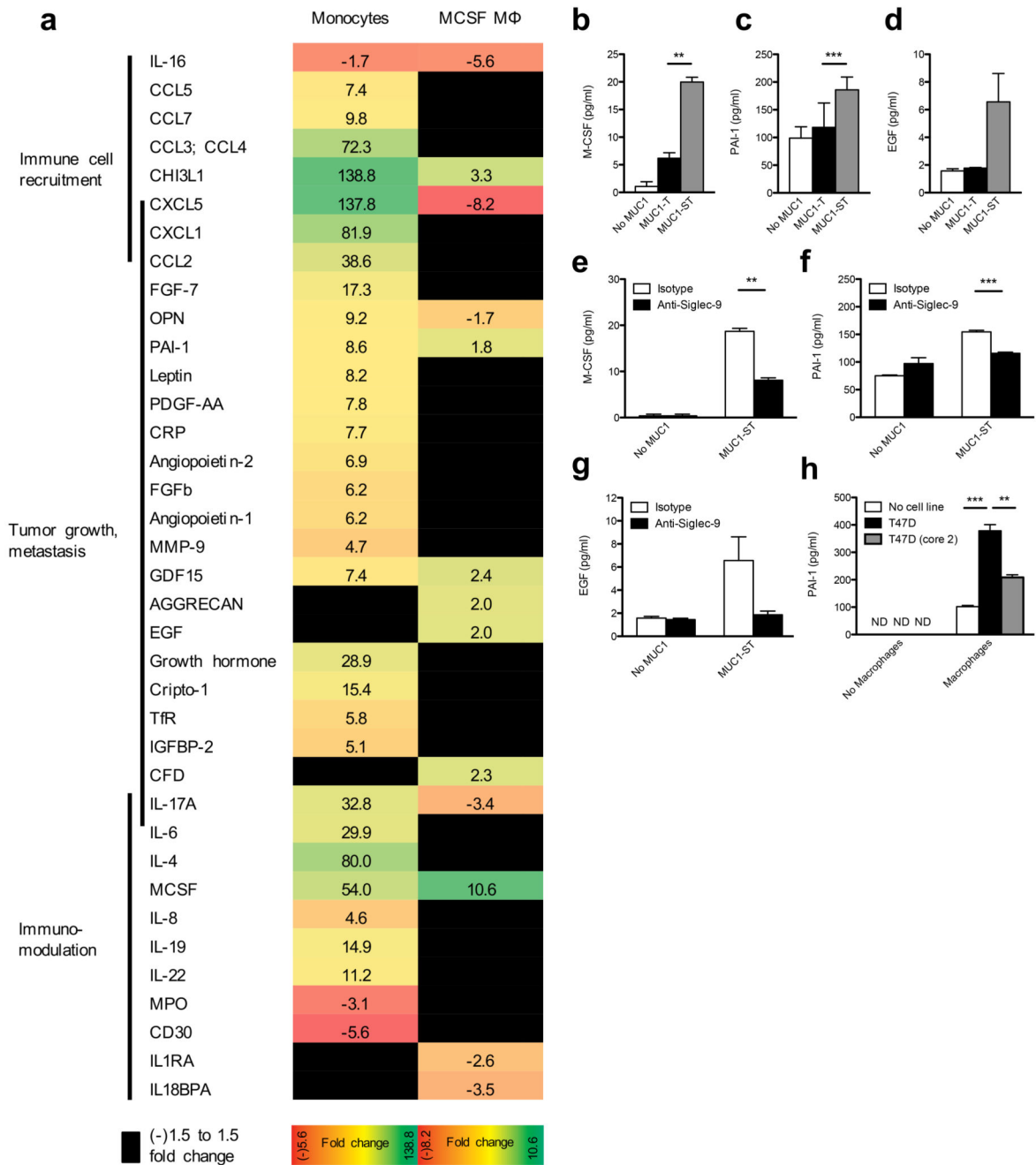


Figure 4. MUC1-ST educated M-CSF macrophages secrete factors associated with tumor progression in a Siglec-9 dependent manner. **(a)** The secretome from monocyte derived M-CSF macrophages treated MUC1-ST clustered into functional groups and compared to the MUC1-ST educated monocyte signature. Figures represent fold change from untreated cells. **(b-g)** Validation by ELISA of M-CSF, PAI-1, EGF released by M-CSF macrophages in response to MUC1-ST, in a sialic acid **(b,c,d)** and Siglec-9 **(e,f,g)** dependent manner. **(h)** PAI-1 secreted by macrophages incubated with T47D cells and as a control T47D cells

engineered to carry normal extended core 2 O-linked glycans (T47D (core 2)). $N=3$ independent donors (**b,c,d,e,f,g**); Representative of 2 independent experiments with the statistical analysis performed on technical triplicates (**h**). Data shown are the mean and s.e.m. $P = ** < 0.01$, $*** 0.001$, as determined by Student's paired t -test (**b,c,d,e,f,g**), or unpaired t -test (**h**).

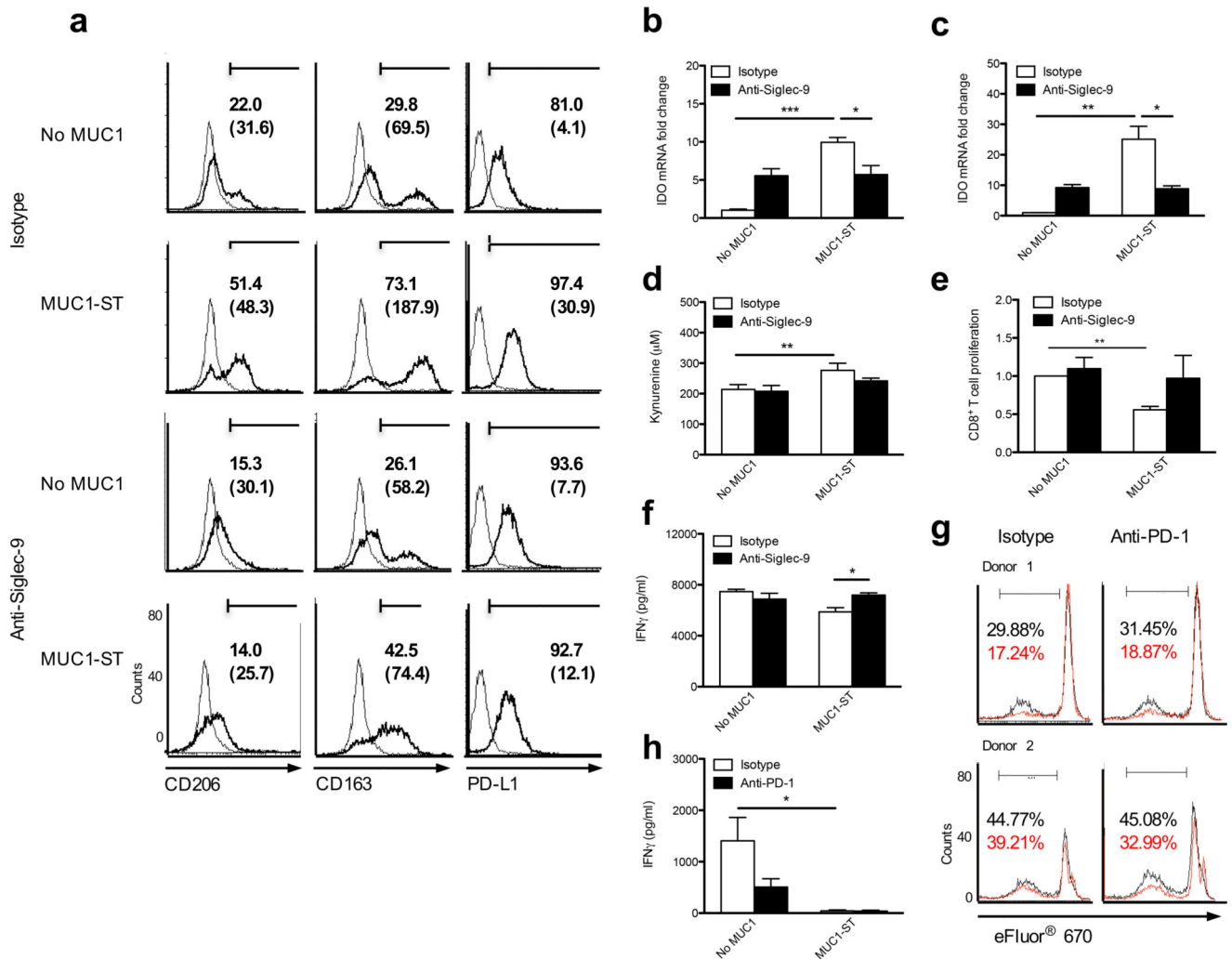


Figure 5. MUC1-ST educated M-CSF macrophages differentiate into tumor-associated macrophages (TAMs). **(a)** Flow cytometry histograms showing CD206, CD163 and PD-L1 expression on macrophages treated with MUC1-ST ± anti Siglec-9 or isotype as indicated. Numbers refer to % positive cells and, in brackets, to corrected MFI. **(b,c)** Normalised (actin) IDO mRNA expression from **(b)** GM-CSF or **(c)** M-CSF macrophages treated with MUC1-ST ± anti Siglec-9 or isotype. Data displayed as fold change with respect to cells treated with isotype control alone. **(d)** Concentration of kynurenine in the supernatant of M-CSF macrophages treated with MUC1-ST ± anti-Siglec-9 or isotype. **(e,f)** M-CSF macrophages treated with MUC1-ST ± anti Siglec-9 or isotype were co-cultured with labeled allogeneic CD8⁺ T cells and **(e)** proliferation or **(f)** IFN γ secretion measured by flow cytometry and ELISA respectively. **(g,h)** M-CSF macrophages treated with MUC1-ST were co-cultured with labeled allogeneic CD8⁺ T cells in the presence of anti-PD-1 (pembrolizumab) or isotype and **(g)** proliferation or **(h)** IFN γ secretion measured by flow cytometry and ELISA respectively. % CD8⁺ T cell proliferative response to allogeneic M-CSF macrophages is shown in black and to MUC1-ST treated allogeneic macrophages in red. Representative

experiment of two giving similar results (**a**); $N=2$ independent experiments with 2 different donors, statistical analysis performed on technical triplicates (**b,c**); $N=4$ independent donors (**d**); $N=3$ independent donors (**e,f**); $N=2$ donors different from 5e (**g**); $N=3$ donors different from 5f (**h**). $P = * < 0.05$, $** < 0.01$, $*** < 0.001$, as determined by Student's paired t -test (**d,e,h**), or unpaired t -test (**b,c,f**).

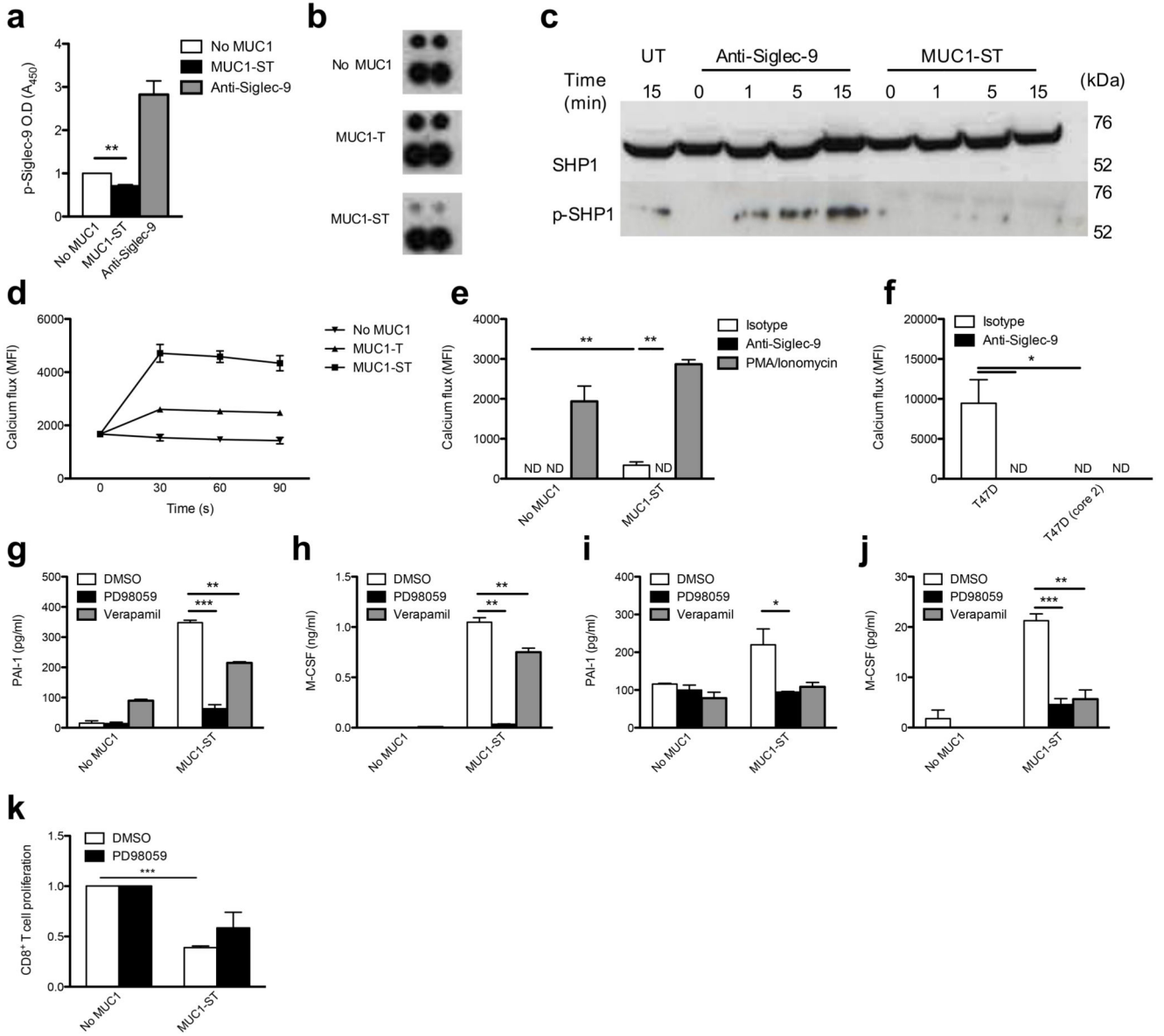


Figure 6.

MUC1-ST binding to myeloid cells via Siglec-9 leads to calcium flux and MEK/ERK activation. (a) Monocytes treated with MUC1-ST or cross-linked anti-Siglec-9 were lysed in the presence of pervanadate and assayed for phospho-Siglec-9. (b) Lysates from M-CSF macrophages treated with MUC1-ST or MUC1-T were assessed for the phosphorylation of Siglec-9 (top, phospho-Siglec-9; bottom, reference). (c) Lysates from MUC1-ST or cross-linked anti-Siglec-9 treated monocytes, were probed for SHP-1 and phospho-SHP-1 (d) Fluorescent calcium reporter labeled monocytes were treated with MUC1-ST or MUC1-T and calcium flux measured. (e) Calcium reporter labeled monocytes were treated with MUC1-ST ± anti-Siglec-9 or isotype or PMA, ionomycin; MFI measured at 60 seconds. (f) Calcium reporter labeled monocytes were co-cultured with T47D cells or T47D(core-2) cells ± anti-Siglec-9 or isotype; MFI measured at 60 seconds. (g,h) Monocytes were treated with

PD98059 or verapamil prior to MUC1-ST. Supernatants were assayed for (g) PAI-1 and (h) M-CSF. (i,j) Macrophages were treated as in g and h and supernatants assayed for (i) PAI-1 and (j) M-CSF. (k) Macrophages treated with MUC1-ST ± PD98059 were incubated with allogeneic labeled CD8⁺ T cells. *N*=3 independent donors (a); Representative of 2 experiments each using different donors (b); Representative of 2 independent donors, the statistical analysis done on technical triplicates (d,f); *N*=3 independent donors (e,g,h,i,j); *N*=2, and the statistical analysis done on pooled duplicates from the two donors (k). Data shown are the mean and s.e.m. *P* =*<0.05, **<0.01, ***0.001, as determined by Student's paired *t*-test (a,e,g,h,i,j), or unpaired *t*-test (f,k).